Comparison of Radon Adsorption on Hematite and Charcoal Activated Powder in Air

Vanja Radolić, Goran Šmit,* Igor Miklavčić, Marina Poje Sovilj

Josip Juraj Strossmayer University of Osijek, Department of Physics, Trg Ljudevita Gaja 6, HR-31000 Osijek, Croatia

* Corresponding author's e-mail address: gsmit@fizika.unios.hr

Abstract: Adsorption of radon in the air was investigated on hematite, α-Fe$_2$O$_3$, and charcoal activated powder. Hematite had almost doubled efficiency in comparison to charcoal activated powder in the same experimental conditions but over a significantly longer period. Adsorption isotherms revealed a typical Langmuir shape on hematite and almost linear on activated charcoal. Linear models of Langmuir, Freundlich and Dubinin-Radushkevich isotherms showed that radon adsorption on both adsorbents is a favourable chemical process, with stronger interactions on hematite, that takes place forming a monolayer of adsorbed radon. The kinetic analysis confirmed forming of a monolayer on both adsorbents and two rate-controlling steps during radon adsorption on hematite, instead of one on activated charcoal, which could be considered as a reason of slower rate of process on hematite.

Keywords: hematite, activated charcoal, radon, adsorption, air.

INTRODUCTION

RADON is a radioactive, colourless, tasteless and odourless gas from the noble gases group which makes it chemically almost inert. Because it is a product of the radioactive decay of radium, and both are members of the uranium series, as gas it can diffuse into the environment from rocks containing these two elements but also through the soil and foundations into buildings. If such buildings are not sufficiently ventilated, then the concentration of radon can increase significantly and exposure of people over a long period of time to such elevated radon levels can cause lung cancer. Charcoal activated powder (activated carbon) and silica gel are often used as a possible protection against increased radon concentration due to diffusion, that is for its removal from the premises where people reside.[1,2] In recent years, new radon replacement adsorbents have also been tested, such as zeolites, *i.e.*, zeolitic imidazole frameworks.[3,4] In addition, activated carbon is also used in one of the methods for the determining the average activity concentration of radon in the air which is in accordance with the International Standard for the Measurement of radioactivity in the environment - Air: radon-222.[5] The intention of this work was to investigate the potential of hematite, α-Fe$_2$O$_3$, as radon adsorbent from air enriched with radon and compare it to adsorption on charcoal activated powder in the same conditions. Namely, it is well known that iron oxides, because of their particular properties, serve as supports in synthesis of different efficient catalysts, model systems in adsorptions and functional materials for radioactive waste management.

EXPERIMENTAL

Adsorbents

As adsorbents were used hematite was prepared in our laboratory and charcoal activated powder QP (PanReac, Spain) as received. Hematite was prepared by heating, previously synthesized,[6] magnetite for 2 h at 873.15 K in the airstream. Figure 1 is an X-ray diffractogram of so prepared hematite which was taken on a Philips 3710 diffractometer operated at 40 kV and 40 mA using monochromatic Cu Kα radiation. The range in 2θ from 10 to 70° was scanned by a speed of 0.02° s^{-1} at room temperature.

Adsorption

Radon adsorption was investigated using the experimental setup shown in Figure 2. The source of radon was crushed uranium ore (Rn) placed in a Petri dish and covered with filter paper. The amount and activity of uranium ore enable the formation and accumulation of radon in the desiccator (D), with a volume of 11.4 dm³, in a concentration range from 5 to 45 kBq m⁻³. So accumulated radon was transported through open valves V_3 and V_4 to the AlphaGUARD ionization chamber (Genitron Instruments, Germany) or back to the desiccator. To stabilize the concentration of radon throughout the setup, with the use of a flow rate of Q = 0.3 dm³ min⁻¹, takes a time of one day. The AlphaGUARD measuring cycle is 10 min in FLOW mode, whereby during one measuring cycle, in addition to the flow used, almost 5 detection volumes of air are exchanged. After stabilizing the radon concentration in the system, valves V_3 and V_4 were closed and V_1 and V_2 were opened, which passes radon-enriched air through the adsorbent (hematite and activated charcoal) located in glass tubes (Figure 3) at a constant temperature of 298.15 K. The mass of both adsorbents was 0.3 g.

The measured radon concentrations, c_{Rn} (expressed in Bq m⁻³), are converted to molar concentrations, $c = n/V$ (expressed in mol m⁻³), as follows. The amount of
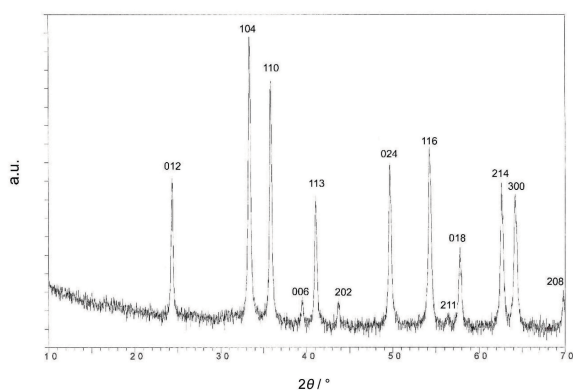

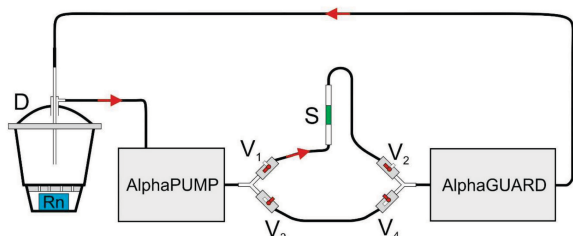**Figure 1.** XRD pattern of hematite used as the adsorbent for radon in air.

Figure 2. Experimental setup for radon adsorption (Rn: crushed uranium ore, S: sample of adsorbent, V: valves, D: desiccator).

Figure 3. Samples of hematite (above) and charcoal activated powder were used as the adsorbents for radon in the air (m = 0.3 g).

radon, n / mol, is defined as:

$$n = \frac{m}{M} \tag{1}$$

where m / g is the radon mass and M is the molar mass of radon (222 g mol⁻¹). The mass of radon can also be determined from:

$$m = \frac{A_{Rn}}{SA} \tag{2}$$

where A_{Rn} / Bq is radon activity and SA / Bq g⁻¹ is specific activity equal to $5.7 \cdot 10^{15}$ Bq g⁻¹ according to the expression:

$$SA = \frac{N_A \cdot \lambda}{M} \tag{3}$$

where N_A is Avogadro constant ($6.022 \cdot 10^{23}$ mol⁻¹) and λ is the decay constant ($2.1 \cdot 10^{-6}$ s⁻¹). Radon activity, A_{Rn}, can be expressed as $c_{Rn} \cdot V$, where V is the volume of the AlphaGUARD ionization chamber ($0.56 \cdot 10^{-3}$ m³). Therefore:

$$C = \frac{c_{Rn}}{N_A \cdot \lambda} \tag{4}$$

These molar concentrations are used as input parameters c_0 (before adsorption), c_e (at the end of adsorption) and c_t (at time t corresponding to the duration of adsorption) for analysis of isotherm and kinetic models of adsorption.

RESULTS AND DISCUSSION

Isotherm Models

Isotherm models give the information about interaction of adsorbates with adsorbents and theoretical maximum adsorption capacity on the basis of the final adsorbed quantity of adsorbate per unit of adsorbent mass on the dependence of its remaining concentration in equilibrium.

The adsorbed amount of radon at the end of adsorption, q_e / mol g⁻¹, is determined as:[7]

$$q_e = \frac{(c_0 - c_e) \cdot V_S}{m_A} \tag{5}$$

where c_0 / mol dm⁻³ is the initial concentration of radon in the air, c_e / mol dm⁻³ is the concentration of radon in air at
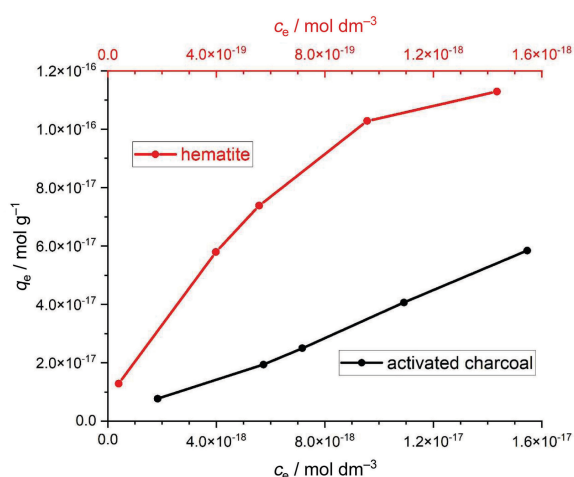
Figure 4. Adsorption isotherms for radon adsorption on hematite and charcoal activated powder (c_0 = 45 kBq m^{-3}).

equilibrium, i.e., at the end of adsorption, V_S / dm^3 is the volume of the system and m_A / g is the mass of adsorbent.

Figure 4 depicts the dependence of radon uptake at hematite and charcoal activated powder of equilibrium radon concentrations. As can be seen, the adsorption isotherm for hematite has a shape of Langmuir type with a characteristic initial increase of the adsorbed radon with an increase of initial radon concentration in the air followed by saturation, caused by limited free sites, and forming an adsorbed monolayer. On the other hand, isotherm for charcoal activated powder has an almost linear shape (R^2 = 0.9954) meaning that q_e is proportional to the initial concentration.

Table 1 presents the parameters of linear Langmuir, Freundlich and Dubinin-Radushkevich adsorption isotherm models.

Linear form used for Langmuir isotherm modelling was:[8]

$$\frac{1}{q_e} = \frac{1}{q_{max} K_L} \cdot \frac{1}{c_e} + \frac{1}{q_{max}} \qquad (6)$$

where q_{max} / mol g^{-1} is the maximum adsorption capacity of the monolayer and K_L / mol^{-1} dm^3 is Langmuir constant which could be assumed as equilibrium constant K considering the fact that it is the actual constant for dynamic equilibrium of:[9]

$$A \text{ (g)} + M \text{ (surface)} \rightleftarrows AM \text{ (surface)}$$
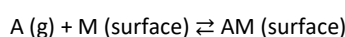
with rate constants k_a for adsorption and k_d for desorption. Hence:

$$K = \frac{k_a}{k_d} \qquad (7)$$

As can be seen, values of q_{max} are almost identical and K_L suggest rather favourable adsorption on both adsorbents.

This is also confirmed with an important feature of the Langmuir isotherm known as the separation factor, R_L:

$$R_L = \frac{1}{1 + K_L \cdot c_0} \qquad (8)$$

Namely, R_L values can very simply characterize adsorption as:[10]

Favourable adsorption: $0 < R_L < 1$,
Unfavourable adsorption: $R_L > 1$,
Irreversible adsorption: $R_L = 0$,
Linear adsorption: $R_L = 1$.

Values are significantly closer to zero in the case of hematite, which is nearly irreversible, indicating stronger interactions[11] with radon in comparison with charcoal activated powder (Figure 5). Also, higher R_L at lower concentrations in both cases implies that adsorption is favourable at lower concentrations[12] and especially on

Table 1. Parameters of Langmuir, Freundlich and Dubinin-Radushkevich adsorption isotherm models.

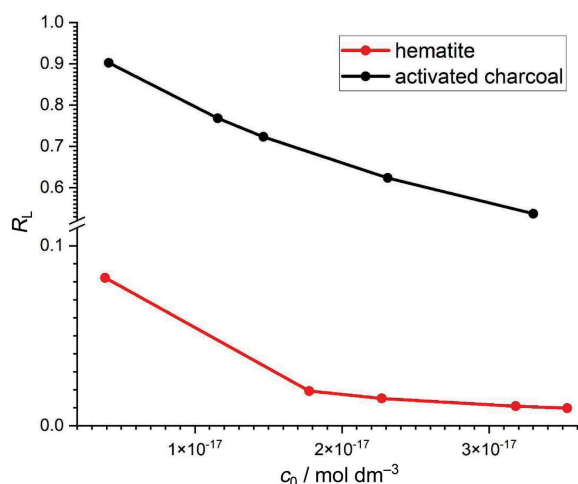| Isotherm model	Parameter	Hematite	Charcoal activated powder
Langmuir	q_{max} / mol g^{-1}	$1.2346 \cdot 10^{-16}$	$1.6667 \cdot 10^{-16}$
	K_L / mol^{-1} dm^3	$2.9136 \cdot 10^{18}$	$2.6086 \cdot 10^{16}$
	R_L	$0.0822 - 9.8151 \cdot 10^{-3}$	$0.9023 - 0.5370$
	R^2	0.9977	0.9930
Freundlich	$1/n_F$	0.6300	0.9500
	K_F / mol g^{-1}	$1.9953 \cdot 10^{-5}$	0.5012
	R^2	0.9936	0.9909
Dubinin-Radushkevich	q_{max} / mol g^{-1}	$2.7967 \cdot 10^{-11}$	$3.0749 \cdot 10^{-9}$
	E / J mol^{-1}	20498.002	16054.032
	R^2	0.9949	0.9893

Figure 5. Separation factors for adsorption of radon on hematite and charcoal activated powder (c_0 = 45 kBq m^{-3}).

activated charcoal considering the final difference between the first and the last value. Linear plot of Freundlich isotherm is obtained by:[12]

$$\log q_e = \log K_F + \frac{1}{n_F} \cdot \log c_e \tag{9}$$

where K_F / mol g^{-1} presents the adsorption capacity of the system with the possibility of forming a multilayer. If $1/n_F$ = 1 it suggests that the adsorption process is linear. If not, then $1/n_F$ is a measure of non-linearity between the concentration and adsorption in such a way that $1/n_F > 1$ implies adsorption as a favourable physical process and if $1/n_F < 1$ adsorption is a chemical process. Values of K_F assume forming of multilayer in both cases, especially on charcoal, but it is not unusual because Freundlich isotherm does not have a defined maximum saturation and, in other words, the adsorbed amount increases infinitely with concentration.[13] Looking at $1/n_F$, one can conclude that adsorption is chemical over hematite and also over charcoal, but that latter value is very close to 1 which is in accordance with Figure 4.

Also, when $1/n_F$ is closer to 0 surface is more heterogeneous like it is on examined hematite. Very high R^2 values in Langmuir and Freundlich models, which are originally quite opposite in approach considering homogeneity of adsorbent surface and layering of adsorbate on that surface, can appear together if heterogeneous surface conditions and monolayer adsorption coexist in applied experimental conditions.[14] Anyway, looking at R^2 values, linear methods of these two models could be used to predict the adsorption process of radon on both adsorbents including also Dubinin-Radushkevich model (Table 1).

In the Dubinin-Radushkevich linear model:[15]

$$\ln q_e = \ln q_{max} - K_{DR} \cdot \varepsilon^2 \tag{10}$$

K_{DR} / J^{-2} mol^2 is the Dubinin-Radushkevich constant related to mean free energy of adsorption per mole of the adsorbate E / J mol^{-1} as:

$$E = \frac{1}{\sqrt{(-2K_{DR})}} \tag{11}$$

and ε / J mol^{-1} is the Polanyi potential:

$$E = RT \ln\left(1 + \frac{1}{c_e}\right) \tag{12}$$

where R is the gas constant (8.314 J K^{-1} mol^{-1}) and T / K is the temperature. The value of E may offer a conclusion about the adsorption mechanism. When its value is in the range of 1−8 kJ mol^{-1}, it supposes physical adsorption. The value of E between 8 and 16 kJ mol^{-1} is attributed to the adsorption process that takes place by the chemical ion-exchange mechanism, while E greater than 16 kJ mol^{-1} indicates chemisorption.[16] So, in both occasions, chemical adsorption occurs but is more intensively over hematite as it is confirmed also with R_L values.

Kinetic Models

Kinetic models of adsorption describe the uptake rate that in turn controls residence time and process mechanisms of the full-scale adsorption. Kinetic data were gained by the variation of concentration of removed radon against time with changing initial concentrations of radon.

The efficiency of adsorbents in removing radon from the air in dependence on time was calculated using the following equation:[17]

$$R / \% = \frac{c_0 - c_t}{c_0} \cdot 100 \tag{13}$$

where R / % is the radon removal efficiency, c_0 / mol dm^{-3} is the initial concentration of radon in air and c_t / mol dm^{-3} is the concentration of radon in air at time t / min corresponding to the duration of adsorption.

Figure 6 shows the efficiency of adsorbents in removing radon from the air with its highest concentration of 45 kBq m^{-3} and it is obvious that hematite is a much better adsorbent with an efficiency to 95 % while activated charcoal reached a bit over 55 % but in a much shorter period.

The adsorbed amount of radon), q_t / mol g^{-1}, at time t / min is determined as:[18]

$$q_t = \frac{(c_0 - c_t) \cdot V_S}{m_A} \tag{14}$$

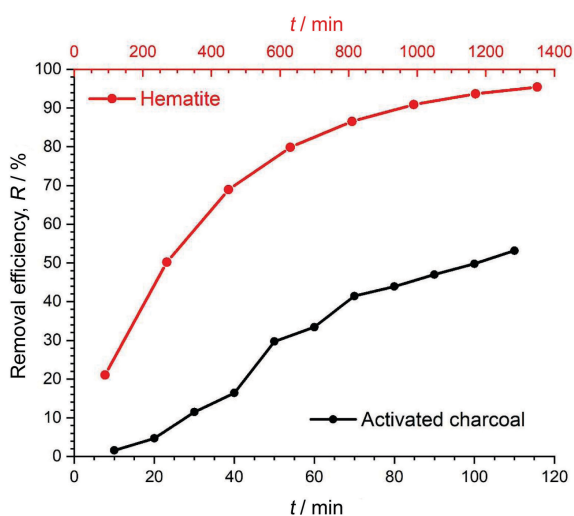where c_0 / mol dm^{-3} is the initial concentration of radon in

Figure 6. Removal efficiencies for adsorption of radon on hematite and charcoal activated powder ($c_0 = 45$ kBq m^{-3}).

air, c_t / mol dm^{-3} is the concentration of radon in air at time t / min, V_S / dm^3 is the volume of the system and m_A / g is the mass of adsorbent. Calculations were presented for measurements with an initial concentration of 45 kBq m^{-3}.

Table 2 presents parameters of linear Elovich, intra-particle, first-order and pseudo-first-order adsorption kinetic models.

Elovich equation, commonly used to determine the kinetics of the chemisorption of gases onto heterogeneous solids at the initial state of adsorption, is:[19]

$$q_t = \frac{1}{\beta} \cdot \ln(t) + \frac{1}{\beta} \cdot \ln(\alpha\beta) \qquad (15)$$

with

α: initial adsorption rate (expressed in mol g^{-1} min^{-1}),
β: desorption constant (expressed in g mol^{-1}) which could be related to the extent of surface coverage and activation energy for chemisorption.[20]

It does not propose any kind of mechanism for adsorption but results revealed a bigger initial adsorption rate over charcoal and almost identical desorption constants which is in accordance with the observed efficiency of these adsorbents against time.

Intra-particle model in linear form is useful for estimation of mechanism as:[21]

$$q_t = k_{id} \cdot t^{\frac{1}{2}} + C \qquad (16)$$

where are

k_{id}: intra-particle diffusion rate constant (expressed in mol g^{-1} min$^{-0.5}$),
C: intercept (expressed in mol g^{-1}) and its value stands for the thickness of the boundary layer.

Namely, the mechanism of adsorption is generally considered to involve three steps, one or any combination of which can be the rate-controlling mechanism:[11]

1. External diffusion to the surface of the adsorbent.
2. Adsorption at sites on the surface (external or internal in pores) which energy depends on the binding process (physical or chemical). This step is often assumed to be extremely rapid so it is not considered as rate-determining.
3. Intra-particle diffusion of the adsorbate molecules to an adsorption site either by a diffusion through the pores or by solid surface diffusion in pores.

Table 2. Parameters of Elovich, intra-particle, first-order and pseudo-first-order adsorption kinetic models.

| Kinetic model	Parameters	Hematite	Charcoal activated powder
Elovich	α / mol g^{-1} min^{-1}	$7.4980 \cdot 10^{-19}$	$1.7083 \cdot 10^{-18}$
	β / mol^{-1} g	$2.8490 \cdot 10^{16}$	$2.9940 \cdot 10^{16}$
	R^2	0.9918	0.9680
Intra-particle	k_{id} / mol g^{-1} min$^{-1/2}$	$5.0300 \cdot 10^{-18}$	$1.0000 \cdot 10^{-17}$
		$1.8100 \cdot 10^{-18}$	
	C / mol g^{-1}	$-2.4400 \cdot 10^{-17}$	$-4.1000 \cdot 10^{-17}$
		$4.9500 \cdot 10^{-17}$	
	R^2	0.9869	0.9800
		0.9730	
First-order	k_1 / min^{-1}	0.00235	0.00894
	R^2	0.9939	0.9800
Pseudo-first-order	k_1 / min^{-1}	0.00312	0.0304
	q_e / mol g^{-1}	$1.2654 \cdot 10^{-16}$	$1.1634 \cdot 10^{-16}$
	R^2	0.9955	0.9767
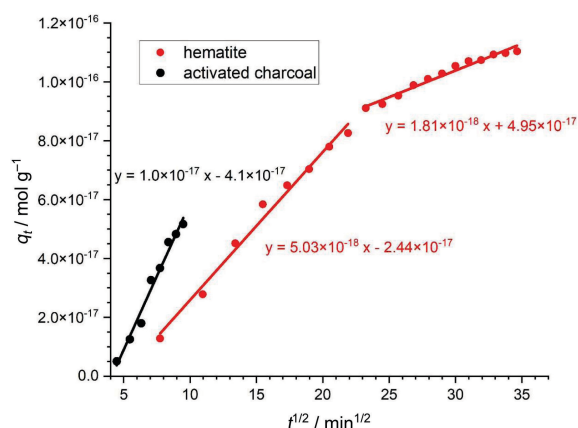
Figure 7. Plots of intra-particle diffusion model for adsorption of radon on hematite and charcoal activated powder (c_0 = 45 kBq m^{-3}).

If the regression of q_t versus $t^{1/2}$ is linear and passes through the origin, then intra-particle diffusion was the sole rate-limiting step and that is almost the case in all three linear trends presented in Table 2 and Figure 7. Namely, in the case of hematite, one cannot ignore the presence of two slightly separated trends where the initial slope could be due to external surface adsorption (instantaneous) while the second one is the gradual adsorption stage where the intraparticle diffusion occurs simultaneously in the adsorption mechanism as the second ratecontrolling step.[21]

So, k_{id} value is a bit larger for charcoal, but hematite has two rate-determining steps instead one.

A kinetic equation based on the influence of concentration of radon in time t (expressed in min) on the rate of the process was used as a linear first-order model:[22]

$$\ln\left(\frac{c_0}{c_t}\right) = k_1 \cdot t \tag{17}$$

k_1: first-order rate constant (expressed in min^{-1})

To distinguish kinetic equation based on concentrations from adsorption capacities of adsorbents, Lagergren's first-order rate,[23] called pseudo-first-order was employed:

$$\ln(q_e - q_t) = \ln q_e - k_1 \cdot t \tag{18}$$

with

q_e: adsorption capacity of Rn at equilibrium (expressed in mol g^{-1}),

q_t: adsorption capacity of Rn at time t (expressed in mol g^{-1}),

k_1: pseudo-first-order rate constant (expressed in min^{-1}).

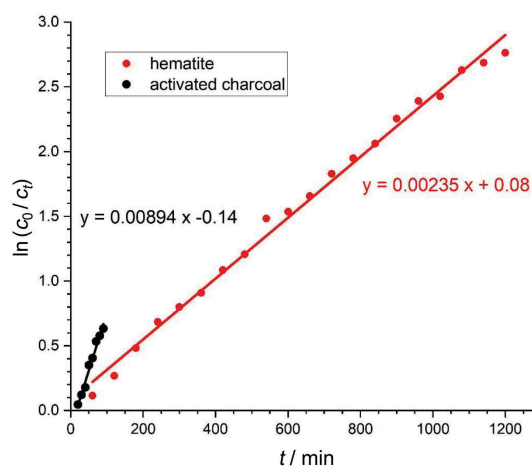Despite small differences in correlation coefficients, all previous observations were confirmed:

Figure 8. Plots of first-order model for adsorption of radon on hematite and charcoal activated powder (c_0 = 45 kBq m^{-3}).
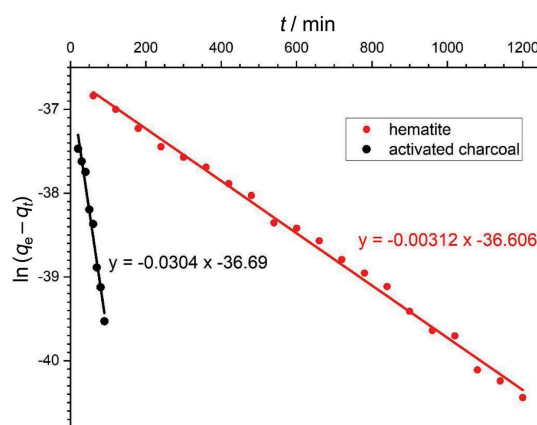

Figure 9. Plots of pseudo-first-order model for adsorption of radon on hematite and charcoal activated powder (c_0 = 45 kBq m^{-3}).

q_e are between themselves approximately equal and in accordance with Langmuir q_{max} implying monolayer in both cases while k_1 values approve faster process on activated charcoal (Figures 8 and 9).

CONCLUSION

Hematite, α-Fe$_2$O$_3$, has great potential as a radon adsorbent in the air with almost doubled efficiency in comparison to charcoal activated powder in the same experimental conditions but in a significantly longer period. In practical applications where volume of used adsorbent plays an important role, hematite would be superior in radon adsorption compared to activated charcoal.

Analysis of isotherm models confirms that radon adsorption on both adsorbents is a favourable chemical process, with stronger interactions on hematite, that takes place forming a monolayer of adsorbed radon.

Forming of monolayer approved also kinetic models, as well as of the larger rate of process over charcoal activated powder because of bigger initial adsorption rate and it has only intraparticle diffusion as rate-determining step instead of two rate-determining steps in radon adsorption on hematite.

Rates of the process were also larger for charcoal considering first-order and pseudo-first-order models bearing in mind that this investigation was not typical adsorption of pure gas and presence of oxygen should not be neglected, especially in the case of hematite.

REFERENCES

[1] N. M. Hassan, T. K. Ghosh, A. L. Hines, S. K. Loyalka, *Sep. Sci. Tech.* **1992**, *27*, 1955–1968.
https://doi.org/10.1080/01496399208019458

[2] W. C. Gaul, D. W. Underhill, *Health Phys.* **2005**, *88*, 371–378.
https://doi.org/10.1097/01.HP.0000152110.01409.3e

[3] I. Bikit, D. Mrdja, K. Bikit, S. Grujic, D. Knezevic, S. Forkapic, U. Kozmidis-Luburic, *Radiat. Meas.* **2015**, *72*, 70–74.
https://doi.org/10.1016/j.radmeas.2014.12.001

[4] X.-W. Wang, T. Yan, J. Wan, L.-F. Zhao, Y. Tu, *Nucl. Sci. Tech.* **2016**, 27:9.
https://doi.org/10.1007/s41365-016-0008-7

[5] International Standard ISO 11665-4:2012(E), *Measurement of radioactivity in the environment-Air: radon-222, Part 4: Integrated measurement method for determining average activity concentration using passive sampling and delayed analysis*, 2012, pp. 20-28.

[6] U. Schwertmann, R. M. Cornell, *Iron Oxides in the Laboratory: Preparation and Characterization*, VCH, Weinheim, **1991**, p. 112.

[7] T. K. Naiya, P. Chowdhury, A. K. Bhattacharya, S. K. Das, *Chem. Eng. J.* **2009**, *148*, 68–79.
https://doi.org/10.1016/j.cej.2008.08.002

[8] R. S. Bose, S. Dey, S. Saha, C. K. Ghosh, M. G. Chaudhuri, *Sustain. Water Resour. Manag.* **2016**, *2*, 143–159.
https://doi.org/10.1007/s40899-016-0045-8

[9] P. Atkins, J. de Paula, *Atkins' Physical Chemistry*, Oxford University Press, Oxford, **2010**, p. 890.

[10] M. Belhachemi, F. Addoun, *Appl. Water Sci.* **2011**, *1*, 111–117.
https://doi.org/10.1007/s13201-011-0014-1

[11] M. Kumar, R. Tamilarasan, *Polish J. Chem. Tech.* **2013**, *15*, 29–39.
https://doi.org/10.2478/pjct-2013-0021

[12] M. Iram, C. Guo, Y. Guan, A. Ishfaq, H. Liu, *J. Hazard. Mater.* **2010**, *181*, 1039–1050.
https://doi.org/10.1016/j.jhazmat.2010.05.119

[13] G. D. Halsey, *Adv. Catal.* **1952**, *4*, 259–269.
https://doi.org/10.1016/S0360-0564(08)60616-1

[14] O. Hamdaoui, *J. Hazard. Mater.* **2006**, *135*, 264–273.
https://doi.org/10.1016/j.jhazmat.2005.11.062

[15] A. Babkin, I. Burakova, A. Burakov, D. Kurnosov, E. Galunin, A. Tkachev, I. Ali, *IOP Conf. Ser.: Mater. Sci. Eng.* **2019**, *693*, 012045.
https://doi.org/10.1088/1757-899X/693/1/012045

[16] U. S. Rashid, A. N. Bezbaruah, *Chemosphere* **2020**, *252*, 126639.
https://doi.org/10.1016/j.chemosphere.2020.126639

[17] Z-x. Chen, X-y. Jin, Z. Chen, M. Megharaj, R. Naidu, *J. Colloid Interf. Sci.* **2011**, *363*, 601–607.
https://doi.org/10.1016/j.jcis.2011.07.057

[18] M. H. Do, N. H. Phan, T. D. Nguyen, T. T. S. Pham, V. K. Nguyen, T. T. T. Vu, T. K. P. Nguyen, *Chemosphere* **2011**, *85*, 1269–1276.
https://doi.org/10.1016/j.chemosphere.2011.07.023

[19] U. A. Edet, A. O. Ifelebuegu, *Processes* **2020**, *8*, 665.
https://doi.org/10.3390/pr8060665

[20] A. Farooq, L. Reinert, J.-M. Levêque, N. Papaiconomou, I. Irfan, L. Duclaux, *Microporous Mesoporous Mater.* **2012**, *158*, 55–63.
https://doi.org/10.1016/j.micromeso.2012.03.008

[21] D. Krishnaiah, C. G. Joseph, S. M. Anisuzzaman, W. M. A. W. Daud, M. Sundang, Y. C. Leow, *Korean J. Chem. Eng.* **2017**, *34*, 1377–1384.
https://doi.org/10.1007/s11814-016-0337-6

[22] K. M. Meera Sheriffa Begum, N. Anantharaman, *Adsorpt. Sci. Technol.* **2009**, *27*, 701–722.
https://doi.org/10.1260/0263-6174.27.7.701

[23] Y.-S. Ho, *J. Hazard. Mater.* **2006**, *136*, 681–689.
https://doi.org/10.1016/j.jhazmat.2005.12.043